Robust determination of the Higgs couplings: Power to the data

Tyler Corbett[*]

C. N. Yang Institute for Theoretical Physics, SUNY at Stony Brook, Stony Brook, New York 11794-3840, USA

O. J. P. Éboli[†]

Instituto de Física, Universidade de São Paulo, Brazil and Institut de Physique Théorique,
CEA-Saclay Orme des Merisiers, 91191 Gif-sur-Yvette, France

J. Gonzalez-Fraile[‡]

Departament d'Estructura i Constituents de la Matèria and ICC-UB, Universitat de Barcelona,
647 Diagonal, E-08028 Barcelona, Spain

M. C. Gonzalez-Garcia[§]

Departament d'Estructura i Constituents de la Matèria, Institució Catalana de Recerca i Estudis Avançats (ICREA),
Universitat de Barcelona, 647 Diagonal, E-08028 Barcelona, Spain and C. N. Yang Institute for Theoretical Physics,
SUNY at Stony Brook, Stony Brook, New York 11794-3840, USA

We study the indirect effects of new physics on the phenomenology of the recently discovered "Higgs-like" particle. In a model-independent framework these effects can be parametrized in terms of an effective Lagrangian at the electroweak scale. In a theory in which the $SU(2)_L \times U(1)_Y$ gauge symmetry is linearly realized they appear at lowest order as dimension-six operators, containing all the standard model fields including the light scalar doublet, with unknown coefficients. We discuss the choice of operator basis which allows us to make better use of all the available data to determine the coefficients of the new operators. We illustrate our present knowledge of those by performing a global five-parameter fit to the existing data which allows simultaneous determination of the Higgs couplings to gluons, electroweak gauge bosons, bottom quarks, and tau leptons. We find that for all scenarios considered the standard model predictions for each individual Higgs coupling and observable are within the corresponding 90% C.L. allowed range, the only exception being the Higgs branching ratio into two photons for the scenario with standard couplings of the Higgs to fermions. We finish by commenting on the implications of the results for unitarity of processes at higher energies.

I. INTRODUCTION

After searching for the Higgs boson for decades, the recent discovery of a new state resembling the standard model (SM) Higgs boson [1–6] at the CERN LHC [7] marks the dawn of the direct exploration of the electroweak symmetry breaking sector. In order to determine whether this new particle is indeed the Higgs boson predicted by the SM we must determine its properties like spin, parity [8], and couplings [9,10], as well as keep searching for further states that might be connected to the electroweak symmetry breaking sector. Moreover, the determination of its couplings can give hints of new physics beyond the SM with some cutoff scale Λ above which the new physics states are expected to appear.

Although we do not know the specific form of this theory which will supersede the SM, we can always parametrize its low-energy effects by means of an effective Lagrangian [11].

The effective Lagrangian approach is a model-independent way to describe new physics, which is expected to manifest itself directly at an energy scale Λ larger than the scale at which the experiments are performed, by including in the Lagrangian higher dimension operators suppressed by powers of Λ. The effective Lagrangian depends on the particle content at low energies, as well as on the symmetries of the low-energy theory.

With the present data we can proceed by assuming that the observed state belongs indeed to a light electroweak doublet scalar and that the $SU(2)_L \otimes U(1)_Y$ symmetry is linearly realized in the effective theory [12–19]. Barring effects associated with violation of total lepton number, the lowest order operators which can be built are of dimension six. The coefficients of these dimension-six operators parametrize our ignorance of the new physics effects in the Higgs phenomenology and our task at hand is to determine them using the available data. This bottom-up approach has the advantage of minimizing the amount of theoretical hypothesis when studying the Higgs couplings.

Following this approach we start by listing in Sec. II the most general set of dimension-six operators which involve

[*]corbett.ts@gmail.com
[†]eboli@fma.if.usp.br
[‡]fraile@ecm.ub.edu
[§]concha@insti.physics.sunysb.edu

triple couplings of the low-energy scalar to the SM gauge bosons and fermions and can affect the present Higgs data. The list is redundant and, at any order, the operators listed are related by the equations of motion (EOM). This allows for a freedom of choice in the election of the basis of operators to be used in the analysis. We will argue in Sec. II C that in the absence of any *a priori* illumination on the form of the new physics the most sensible choice of basis should contain operators whose coefficients are more easily related to existing data from other well tested sectors of the theory. This will reduce to six the number of operators testable with an analysis of the existing Higgs data. We proceed then to briefly describe in Sec. III the technical details of such analysis. The status of this exercise with the most up-to-date experimental results is presented in Sec. IV which updates the analysis in Ref. [9] also extending the previous analysis by including modifications of the Higgs couplings to fermions. We summarize our conclusions in Sec. V.

II. EFFECTIVE LAGRANGIAN FOR HIGGS INTERACTIONS

In order to probe the Higgs couplings we parametrize the deviations from the SM predictions in terms of effective Lagrangians. Here, we assume that the low-energy theory exhibits all the symmetries of the SM and that it contains only the SM degrees of freedom. Furthermore, we consider that the recently observed state belongs to an $SU(2)_L$ doublet.[1] We further assume that the present precision of the data allows us to parametrize the deviations from the SM predictions by operators of dimension up to six, i.e.,

$$\mathcal{L}_{\text{eff}} = \sum_n \frac{f_n}{\Lambda^2} \mathcal{O}_n, \tag{1}$$

where the dimension-six operators $\mathcal{O}_n$ involve gauge boson, Higgs boson, and/or fermionic fields with couplings f_n and where Λ is a characteristic scale. Moreover, we assumed the $SU(3)_c \otimes SU(2)_L \otimes U(1)_Y$ SM local symmetry, as well as the $\mathcal{O}_n$ operators to be P and C even and the conservation of baryon and lepton numbers.

Our first task is to fix the basis of dimension-six operators that is suitable to study the Higgs couplings. Of all dimension-six operators just 59 of them, up to flavor and Hermitian conjugation, are enough to generate the most general S-matrix elements consistent with the above symmetries [20]. Before deciding the operators used in our analyses, let us discuss the dimension-six effective interactions that modify the Higgs coupling to gauge bosons and to fermions.

A. Higgs interactions with gauge bosons

There are eight P and C even dimension-six operators that modify the Higgs couplings to the electroweak gauge bosons, while there is just one operator containing gluons [12,13]:

$$
\begin{aligned}
\mathcal{O}_{GG} &= \Phi^\dagger \Phi G^a_{\mu\nu} G^{a\mu\nu}, & \mathcal{O}_{WW} &= \Phi^\dagger \hat{W}_{\mu\nu} \hat{W}^{\mu\nu} \Phi, & \mathcal{O}_{BB} &= \Phi^\dagger \hat{B}_{\mu\nu} \hat{B}^{\mu\nu} \Phi, \\
\mathcal{O}_{BW} &= \Phi^\dagger \hat{B}_{\mu\nu} \hat{W}^{\mu\nu} \Phi, & \mathcal{O}_W &= (D_\mu \Phi)^\dagger \hat{W}^{\mu\nu} (D_\nu \Phi), & \mathcal{O}_B &= (D_\mu \Phi)^\dagger \hat{B}^{\mu\nu} (D_\nu \Phi), \\
\mathcal{O}_{\Phi,1} &= (D_\mu \Phi)^\dagger \Phi \Phi^\dagger (D^\mu \Phi), & \mathcal{O}_{\Phi,2} &= \frac{1}{2} \partial^\mu (\Phi^\dagger \Phi) \partial_\mu (\Phi^\dagger \Phi), & \mathcal{O}_{\Phi,4} &= (D_\mu \Phi)^\dagger (D^\mu \Phi)(\Phi^\dagger \Phi),
\end{aligned}
\tag{2}
$$

where we denoted the Higgs doublet by Φ and its covariant derivative is $D_\mu \Phi = (\partial_\mu + i\frac{1}{2}g'B_\mu + ig\frac{\sigma_a}{2}W^a_\mu)\Phi$ in our conventions. The hatted field strengths are defined as $\hat{B}_{\mu\nu} = i\frac{g'}{2}B_{\mu\nu}$ and $\hat{W}_{\mu\nu} = i\frac{g}{2}\sigma^a W^a_{\mu\nu}$. Moreover, we denote the $SU(2)_L$ ($U(1)_Y$) gauge coupling as g (g') and the Pauli matrices as σ^a. Our conventions are such that

$$
\begin{aligned}
W^\pm_\mu &= \frac{1}{\sqrt{2}}(W^1_\mu \mp iW^2_\mu), \\
Z^{\text{SM}}_\mu &= \frac{1}{\sqrt{g^2 + g'^2}}(gW^3_\mu - g'B_\mu), \quad \text{and} \\
A^{\text{SM}}_\mu &= \frac{1}{\sqrt{g^2 + g'^2}}(g'W^3_\mu + gB_\mu).
\end{aligned}
\tag{3}
$$

In the unitary gauge the Higgs field is written as

$$\Phi = \frac{1}{\sqrt{2}} \begin{pmatrix} 0 \\ v + h(x) \end{pmatrix}, \tag{4}$$

where v is its vacuum expectation value.

For the sake of completeness of our discussion, it is interesting to introduce the operator that contains exclusively Higgs fields

$$\mathcal{O}_{\Phi,3} = \frac{1}{3}(\Phi^\dagger \Phi)^3 \tag{5}$$

that gives an additional contribution to the Higgs potential

$$\mu_0^2(\Phi^\dagger \Phi) + \lambda_0(\Phi^\dagger \Phi)^2 - \frac{f_{\Phi,3}}{3\Lambda^2}(\Phi^\dagger \Phi)^3. \tag{6}$$

This effective operator leads to a shift of the minimum of the Higgs potential with respect to the SM result

$$v^2 = -\frac{\mu_0^2}{\lambda_0}\left(1 + \frac{v^2}{4\Lambda^2}\frac{f_{\Phi,3}}{\lambda_0}\right) \equiv v_0^2\left(1 + \frac{v^2}{4\Lambda^2}\frac{f_{\Phi,3}}{\lambda_0}\right). \tag{7}$$

---

[1]This implies that the new physics decouples when the cutoff $\Lambda \to \infty$.

The operators $\mathcal{O}_{\Phi,1}$, $\mathcal{O}_{\Phi,2}$, and $\mathcal{O}_{\Phi,4}$ contribute to the kinetic energy of the Higgs boson field h so we need to introduce a finite wave function renormalization in order to bring the Higgs kinetic term to the canonical form

$$H = h\left[1 + \frac{v^2}{2\Lambda^2}(f_{\Phi,1} + 2f_{\Phi,2} + f_{\Phi,4})\right]^{1/2}. \quad (8)$$

Furthermore, the operators $\mathcal{O}_{\Phi,j}$ ($j = 1, 2, 3, 4$) also alter the Higgs mass according to

$$M_H^2 = 2\lambda_0 v^2\left[1 - \frac{v^2}{2\Lambda^2}\left(f_{\Phi,1} + 2f_{\Phi,2} + f_{\Phi,4} + \frac{f_{\Phi,3}}{\lambda_0}\right)\right],$$

where we have expanded to linear order in the f_i coefficients.

The operator $\mathcal{O}_{BW}$ contributes at tree level to $Z\gamma$ mixing; therefore, the mass eigenstates are

$$Z_\mu = \left[1 + \frac{2gg'}{g^2 + g'^2}\frac{v^2}{\Lambda^2}f_{BW}\right]^{-1/2}Z_\mu^{\text{SM}}, \quad (9)$$

$$A_\mu = \left[1 - \frac{2gg'}{g^2 + g'^2}\frac{v^2}{\Lambda^2}f_{BW}\right]^{-1/2}A_\mu^{\text{SM}} + \left[\frac{g^2 - g'^2}{g^2 + g'^2}\frac{v^2}{\Lambda^2}f_{BW}\right]^{-1}Z_\mu^{\text{SM}}. \quad (10)$$

The operators $\mathcal{O}_{BW}$, $\mathcal{O}_{\Phi,1}$, $\mathcal{O}_{\Phi,3}$, and $\mathcal{O}_{\Phi,4}$ also have an impact on the electroweak gauge boson masses. Expanding to linear order in the f_i coefficients they read

$$M_Z^2 = \frac{g^2 + g'^2}{4}v^2\left[1 + \frac{v^2}{2\Lambda^2}\left(f_{\Phi,1} + f_{\Phi,4}\right. \right. \\ \left. \left. + \frac{2gg'}{g^2 + g'^2}\frac{v^2}{\Lambda^2}f_{BW}\right)\right], \quad (11)$$

$$M_W^2 = \frac{g^2}{4}v^2\left[1 + \frac{v^2}{2\Lambda^2}f_{\Phi,4}\right] \\ = \frac{g^2}{4}v_0^2\left[1 + \frac{v^2}{2\Lambda^2}\left(f_{\Phi,4} + \frac{f_{\Phi_3}}{2\lambda_0}\right)\right]. \quad (12)$$

Notice that $\mathcal{O}_{BW}$ and $\mathcal{O}_{\Phi,1}$ contribute to the Z mass but not to the W mass, therefore violating the custodial $SU(2)$ symmetry and contributing to T (or $\Delta\rho$).

In our calculations we will always use as inputs the measured values of G_F, M_Z, and α, where the electromagnetic coupling is evaluated at zero momentum. Furthermore, when convenient, we will also absorb part of the tree-level renormalization factors by using the measured value of M_W. In particular using $\frac{G_F}{\sqrt{2}} = \frac{g^2}{8M_W^2}$ and Eqs. (11) and (12) we obtain that

$$v = (\sqrt{2}G_F)^{-1/2}\left(1 - \frac{v^2}{4\Lambda^2}f_{\Phi,4}\right), \quad (13)$$

$$M_Z^2 = (\sqrt{2}G_F)^{-1}\frac{1}{c^2}\left(1 + \frac{v^2}{2\Lambda^2}f_{\Phi,1} + \frac{2gg'}{g^2 + g'^2}\frac{v^2}{\Lambda^2}f_{BW}\right), \quad (14)$$

where we have denoted by $c \equiv g/\sqrt{g^2 + g'^2}$ the tree-level cosine of the SM weak mixing angle.

The dimension-six effective operators in Eq. (2) give rise to Higgs interactions with SM gauge boson pairs that take the following form in the unitary gauge:

$$\mathcal{L}_{\text{eff}}^{\text{HVV}} = g_{Hgg}HG_{\mu\nu}^a G^{a\mu\nu} + g_{H\gamma\gamma}HA_{\mu\nu}A^{\mu\nu} \\ + g_{HZ\gamma}^{(1)}A_{\mu\nu}Z^\mu\partial^\nu H + g_{HZ\gamma}^{(2)}HA_{\mu\nu}Z^{\mu\nu} \\ + g_{HZZ}^{(1)}Z_{\mu\nu}Z^\mu\partial^\nu H + g_{HZZ}^{(2)}HZ_{\mu\nu}Z^{\mu\nu} \\ + g_{HZZ}^{(3)}HZ_\mu Z^\mu + g_{HWW}^{(1)}(W_{\mu\nu}^+W^{-\mu}\partial^\nu H + \text{H.c.}) \\ + g_{HWW}^{(2)}HW_{\mu\nu}^+W^{-\mu\nu} + g_{HWW}^{(3)}HW_\mu^+W^{-\mu}, \quad (15)$$

where $V_{\mu\nu} = \partial_\mu V_\nu - \partial_\nu V_\mu$ with $V = A, Z, W$, and G. The effective couplings g_{Hgg}, $g_{H\gamma\gamma}$, $g_{HZ\gamma}^{(1,2)}$, $g_{HWW}^{(1,2,3)}$, and $g_{HZZ}^{(1,2,3)}$ are related to the coefficients of the operators appearing in (1) through

$$g_{Hgg} = \frac{f_{GG}v}{\Lambda^2} \equiv -\frac{\alpha_s}{8\pi}\frac{f_g v}{\Lambda^2},$$

$$g_{H\gamma\gamma} = -\left(\frac{g^2 v s^2}{2\Lambda^2}\right)\frac{f_{BB} + f_{WW} - f_{BW}}{2},$$

$$g_{HZ\gamma}^{(1)} = \left(\frac{g^2 v}{2\Lambda^2}\right)\frac{s(f_W - f_B)}{2c},$$

$$g_{HZ\gamma}^{(2)} = \left(\frac{g^2 v}{2\Lambda^2}\right)\frac{s[2s^2 f_{BB} - 2c^2 f_{WW} + (c^2 - s^2)f_{BW}]}{2c},$$

$$g_{HZZ}^{(1)} = \left(\frac{g^2 v}{2\Lambda^2}\right)\frac{c^2 f_W + s^2 f_B}{2c^2},$$

$$g_{HZZ}^{(2)} = -\left(\frac{g^2 v}{2\Lambda^2}\right)\frac{s^4 f_{BB} + c^4 f_{WW} + c^2 s^2 f_{BW}}{2c^2},$$

$$g_{HZZ}^{(3)} = \left(\frac{g^2 v}{4c^2}\right)\left[1 + \frac{v^2}{4\Lambda^2}\left(3f_{\Phi,1} + 3f_{\Phi,4} - 2f_{\Phi,2}\right. \right. \\ \left. \left. + \frac{2gg'}{g^2 + g'^2}\frac{v^2}{\Lambda^2}f_{BW}\right)\right] \\ = M_Z^2(\sqrt{2}G_F)^{1/2}\left[1 + \frac{v^2}{4\Lambda^2}(f_{\Phi,1} + 2f_{\Phi,4} - 2f_{\Phi,2})\right],$$

$$g_{HWW}^{(1)} = \left(\frac{g^2 v}{2\Lambda^2}\right)\frac{f_W}{2},$$

$$g_{HWW}^{(2)} = -\left(\frac{g^2 v}{2\Lambda^2}\right)f_{WW},$$

$$g_{HWW}^{(3)} = \left(\frac{g^2 v}{2}\right)\left[1 + \frac{v^2}{4\Lambda^2}(3f_{\Phi,4} - f_{\Phi,1} - 2f_{\Phi,2})\right] \\ = 2M_W^2(\sqrt{2}G_F)^{1/2}\left[1 + \frac{v^2}{4\Lambda^2}(2f_{\Phi,4} - f_{\Phi,1} - 2f_{\Phi,2})\right], \quad (16)$$

where $s \equiv g'/\sqrt{g^2 + g'^2}$ stands for the tree-level sine of the SM weak mixing angle. For convenience, we rescaled the coefficient f_{GG} of the gluon-gluon operator by a loop factor $-\alpha_s/(8\pi)$ such that an anomalous gluon-gluon coupling $f_g \sim \mathcal{O}(1\text{–}10)$ gives a contribution comparable to the SM top loop. Furthermore, we have kept the normalization commonly used in the pre-LHC studies for the

operators involving electroweak gauge bosons. Notice that the general expressions above reproduce in the different cases considered those of Refs. [16,18,21].

B. Higgs interactions with fermions

The dimension-six operators modifying the Higgs interactions with fermion pairs are

$$
\begin{aligned}
\mathcal{O}_{e\Phi,ij} &= (\Phi^\dagger \Phi)(\bar{L}_i \Phi e_{R_j}), & \mathcal{O}^{(1)}_{\Phi L,ij} &= \Phi^\dagger (i\overleftrightarrow{D}_\mu \Phi)(\bar{L}_i \gamma^\mu L_j), & \mathcal{O}^{(3)}_{\Phi L,ij} &= \Phi^\dagger (i\overleftrightarrow{D}^a_\mu \Phi)(\bar{L}_i \gamma^\mu \sigma_a L_j), \\
\mathcal{O}_{u\Phi,ij} &= (\Phi^\dagger \Phi)(\bar{Q}_i \tilde{\Phi} u_{R_j}), & \mathcal{O}^{(1)}_{\Phi Q,ij} &= \Phi^\dagger (i\overleftrightarrow{D}_\mu \Phi)(\bar{Q}_i \gamma^\mu Q_j), & \mathcal{O}^{(3)}_{\Phi Q,ij} &= \Phi^\dagger (i\overleftrightarrow{D}^a_\mu \Phi)(\bar{Q}_i \gamma^\mu \sigma_a Q_j), \\
\mathcal{O}_{d\Phi,ij} &= (\Phi^\dagger \Phi)(\bar{Q}_i \Phi d_{R_j}), & \mathcal{O}^{(1)}_{\Phi e,ij} &= \Phi^\dagger (i\overleftrightarrow{D}_\mu \Phi)(\bar{e}_{R_i} \gamma^\mu e_{R_j}), & \\
& & \mathcal{O}^{(1)}_{\Phi u,ij} &= \Phi^\dagger (i\overleftrightarrow{D}_\mu \Phi)(\bar{u}_{R_i} \gamma^\mu u_{R_j}), & \\
& & \mathcal{O}^{(1)}_{\Phi d,ij} &= \Phi^\dagger (i\overleftrightarrow{D}_\mu \Phi)(\bar{d}_{R_i} \gamma^\mu d_{R_j}), & \\
& & \mathcal{O}^{(1)}_{\Phi ud,ij} &= \tilde{\Phi}^\dagger (i\overleftrightarrow{D}_\mu \Phi)(\bar{u}_{R_i} \gamma^\mu d_{R_j}), &
\end{aligned}
\tag{17}
$$

where we define $\tilde{\Phi} = \sigma_2 \Phi^*$, $\Phi^\dagger \overleftrightarrow{D}_\mu \Phi = \Phi^\dagger D_\mu \Phi - (D_\mu \Phi)^\dagger \Phi$, and $\Phi^\dagger \overleftrightarrow{D}^a_\mu \Phi = \Phi^\dagger \sigma^a D_\mu \Phi - (D_\mu \Phi)^\dagger \sigma^a \Phi$. We use the notation of L for the lepton doublet, Q for the quark doublet, and f_R for the $SU(2)$ singlet fermions, where i, j are family indices. Notice that, unlike the Higgs-gauge boson operators of the previous subsection, not all Higgs-fermion operators listed above are Hermitian.

In Eq. (17) we have classified the operators according to the number of Higgs fields they contain. In a first set, which we denote $\mathcal{O}_{f\Phi}$, the operators exhibit three Higgs fields and after spontaneous symmetry breaking they lead to modifications of the SM Higgs Yukawa couplings. The second set, $\mathcal{O}^{(1)}_{\Phi f}$, contains operators presenting two Higgs fields and one covariant derivative, and consequently, they contribute to Higgs couplings to fermion pairs which also modify the neutral current weak interactions of the corresponding fermions. The third set, $\mathcal{O}^{(3)}_{\Phi f}$, similar to the second, also leads to modifications of the fermionic charged current interactions.

Operators $\mathcal{O}_{f\Phi,ij}$ renormalize fermion masses and mixing, as well as modify the Yukawa interactions. In the SM, these interactions take the form

$$
\mathcal{L}_{Yuk} = -y^e_{ij} \bar{L}_i \Phi e_{Rj} - y^d_{ij} \bar{Q}_i \Phi d_{Rj} - y^u_{ij} \bar{Q}_i \tilde{\Phi} u_{Rj} + \text{H.c.},
\tag{18}
$$

while the dimension-six modifications of the Yukawa interactions are

$$
\mathcal{L}^{Hqq}_{\text{eff}} = \frac{f_{d\Phi,ij}}{\Lambda^2} \mathcal{O}_{d\Phi,ij} + \frac{f_{u\Phi,ij}}{\Lambda^2} \mathcal{O}_{u\Phi,ij} + \frac{f_{e\Phi,ij}}{\Lambda^2} \mathcal{O}_{e\Phi,ij} + \text{H.c.},
\tag{19}
$$

where a sum over the three families i, $j = 1$, 2, 3 is understood. After spontaneous symmetry breaking and prior to the finite Higgs wave function renormalization in

Eqs. (8), (18), and (19) can be conveniently decomposed in two pieces $\mathcal{L}_0$ and $\mathcal{L}_1$ given by

$$
\begin{aligned}
\mathcal{L}_0 = &\frac{1}{\sqrt{2}} \bar{d}_L \left(-y^d + \frac{v^2}{2\Lambda^2} f_{d\Phi} \right) d_R (v + h) \\
&+ \frac{1}{\sqrt{2}} \bar{u}_L \left(-y^u + \frac{v^2}{2\Lambda^2} f_{u\Phi} \right) u_R (v + h) \\
&+ \frac{1}{\sqrt{2}} \bar{e}_L \left(-y^u + \frac{v^2}{2\Lambda^2} f_{e\Phi} \right) e_R (v + h) + \text{H.c.,}
\end{aligned}
\tag{20}
$$

and

$$
\begin{aligned}
\mathcal{L}_1 = &\frac{1}{\sqrt{2}} \frac{v^2}{\Lambda^2} \bar{d}_L f_{d\Phi} d_R h + \frac{1}{\sqrt{2}} \frac{v^2}{\Lambda^2} \bar{u}_L f_{u\Phi} u_R h \\
&+ \frac{1}{\sqrt{2}} \frac{v^2}{\Lambda^2} \bar{u}_L f_{u\Phi} u_R h + \text{H.c.,}
\end{aligned}
\tag{21}
$$

where $f_{L,R} = (f_{L,R1}, f_{L,R2}, f_{L,R3})^T$ with $f = u$, or d or e and y^f and $f_{f\Phi}$ are 3×3 matrices in generation space.

$\mathcal{L}_0$ is proportional to the mass term for the fermions and in the mass basis leads to the SM-like Higgs-fermion interactions with renormalized fermion masses and quark weak mixings.[2] On the other hand, generically, the new interactions contained in $\mathcal{L}_1$ are not necessarily flavor diagonal in the mass basis unless $f_{f\Phi} \propto y^f$.

Altogether the $H\bar{f}f$ couplings in the fermion mass basis and after renormalization of the Higgs wave function in Eq. (8) can be written as

$$
\mathcal{L}^{Hff} = g^f_{Hij} \bar{f}'_L f'_R H + \text{H.c.}
\tag{22}
$$

---

[2]Since we are not adding right-handed neutrinos to the fermion basis nor allowing for L violating dimension-five operators, the couplings to the charged leptons can be chosen to be generation diagonal in the mass basis as in the SM.

with

$$g^f_{Hij} = -\frac{m^f_i}{v}\delta_{ij}\left[1 - \frac{v^2}{4\Lambda^2}(f_{\Phi,1} + 2f_{\Phi,2} + f_{\Phi,4})\right]$$
$$+ \frac{v^2}{\sqrt{2}\Lambda^2}f'_{f\Phi,ij}, \qquad (23)$$

where we denoted the physical masses by m^f_j and $f'_{q\Phi,ij}$ are the coefficients of the corresponding operators in the mass basis. In what follows we will denote all these coefficients without the prime.

C. The right of choice

In the effective Lagrangian framework not all operators at a given order are independent as they can be related by the use of the classical EOM of the SM fields. The invariance of the physical observables under the associated operator redefinitions is guaranteed as it has been proved that operators connected by the EOM lead to the same S-matrix elements [22]. In a top-bottom approach, when starting from the full theory and integrating out heavy degrees of freedom to match the coefficients of the higher dimension operators at low energies it is convenient not to choose a minimal set of operators in order to guarantee that the operators generated by the underlying theory can be easily identified [23]. However, in a bottom-up approach when we use the effective Lagrangian approach to obtain bounds on generic extensions of the SM, we must choose a minimum operator basis to avoid parameters' combinations that cannot be probed.

In our case at hand, we have to take into account the SM EOM which imply that not all the operators in Eqs. (2) and (17) are independent. In particular the EOM for the Higgs field and the electroweak gauge bosons lead to three relations between the operators:

$$2\mathcal{O}_{\Phi,2} - 2\mathcal{O}_{\Phi,4}$$
$$= \sum_{ij}(y^e_{ij}\mathcal{O}_{e\Phi,ij} + y^u_{ij}\mathcal{O}_{u\Phi,ij} + y^d_{ij}(\mathcal{O}_{d\Phi,ij})^\dagger + \text{H.c.}), \quad (24)$$

$$2\mathcal{O}_B + \mathcal{O}_{BW} + \mathcal{O}_{BB} + g'^2\left(\mathcal{O}_{\Phi,1} - \frac{1}{2}\mathcal{O}_{\Phi,2}\right)$$
$$= -\frac{g'^2}{2}\sum_i\left(-\frac{1}{2}\mathcal{O}^{(1)}_{\Phi L,ii} + \frac{1}{6}\mathcal{O}^{(1)}_{\Phi Q,ii} - \mathcal{O}^{(1)}_{\Phi e,ii}\right.$$
$$\left. + \frac{2}{3}\mathcal{O}^{(1)}_{\Phi u,ii} - \frac{1}{3}\mathcal{O}^{(1)}_{\Phi d,ii}\right), \qquad (25)$$

$$2\mathcal{O}_W + \mathcal{O}_{BW} + \mathcal{O}_{WW} + g^2\left(\mathcal{O}_{\Phi,4} - \frac{1}{2}\mathcal{O}_{\Phi,2}\right)$$
$$= -\frac{g^2}{4}\sum_i(\mathcal{O}^{(3)}_{\Phi L,ii} + \mathcal{O}^{(3)}_{\Phi Q,ii}). \qquad (26)$$

These constraints allow for the elimination of three operators listed in Eqs. (2) and (17).

At this point we are faced with the decision of which operators to leave in the basis to be used in the analysis of the Higgs data; different approaches can be followed in doing so. Again, in a top-bottom approach in which some *a priori* knowledge is assumed about the beyond the SM theory one can use this theoretical prejudice to choose the basis. For example if the UV completion of the SM is a given gauge theory, it is possible to predict whether a given operator is generated at tree level or at loop level [24]. One may then be tempted to keep those in the basis as larger coefficients are expected [21]. However, in the absence of such illumination it is impossible to know if the low-energy theory would contain any tree-level generated operator; for instance see Ref. [25] for a model whose low-energy theory contains only loop induced operators. Furthermore, caution should be used when translating the bounds on the effective operators into the scale of the new physics since after the use of EOM coefficients of operators generated at loop level can, in fact, originate from tree-level operators eliminated using the EOM and vice versa [23]. In fact, all choices of basis suffer from this problem.

In principle, given the proof of the equivalence of the S-matrix elements the determination of physical observables like production cross sections or decay branching ratios would be independent of the choice of basis. Nevertheless independent does not mean equivalent in real life. For this reason in this work we advocate that in the absence of theoretical prejudices it turns out to be beneficial to use a basis chosen by the data: "power to the data." With this we mean that the sensible (and certainly technically convenient) choice is to leave in the basis to be used to study Higgs results those operators which are more directly related to the existing data, in particular to the bulk of precision electroweak measurements which have helped us to establish the SM.

In this approach we choose to retain the fermionic operators in Eq. (17) since they contribute to processes well measured like Z properties at the pole, W decays, low-energy ν scattering, atomic parity violation, flavor-changing neutral currents, parity violation in Moller scattering, and $e^+e^- \rightarrow f\bar{f}$ at LEP2. These processes lead to strong constraints on many of the fermionic operators in our basis [26].

Some of the operators in Eq. (2) contribute at tree level to electroweak precision measurements. In fact, the operators $\mathcal{O}_{\Phi,1}$ and $\mathcal{O}_{BW}$ contribute at tree level to the S and T parameters [14,15,25,27]

$$\alpha\Delta S = e^2\frac{v^2}{\Lambda^2}f_{BW} \text{ and } \alpha\Delta T = \frac{1}{2}\frac{v^2}{\Lambda^2}f_{\Phi,1}. \quad (27)$$

For this reason we keep $\mathcal{O}_{\Phi,1}$ and $\mathcal{O}_{BW}$ in our operator basis.

Presently there is also data on triple electroweak gauge boson vertices [28,29] that should be considered in the choice of basis. The operators $\mathcal{O}_B$ and $\mathcal{O}_W$ modify the

triple gauge-boson couplings $\gamma W^+ W^-$ and $Z W^+ W^-$ that can be parametrized as [15,17]

$$\mathcal{L}_{WWV} = -i g_{WWV} \left\{ g_1^V (W_{\mu\nu}^+ W^{-\mu} V^\nu - W_\mu^+ V_\nu W^{-\mu\nu}) \right.$$
$$\left. + \kappa_V W_\mu^+ W_\nu^- V^{\mu\nu} + \frac{\lambda_V}{m_W^2} W_{\mu\nu}^+ W^{-\nu\rho} V_\rho{}^\mu \right\}, \quad (28)$$

where $g_{WW\gamma} = e = gs$, $g_{WWZ} = gc$. In general these vertices involve six dimensionless couplings [27] g_1^V, κ_V, and λ_V ($V = \gamma$ or Z). Notwithstanding, the electromagnetic gauge invariance requires that $g_1^\gamma = 1$, while the three remaining couplings are related to the dimension-six operators $\mathcal{O}_B$ and $\mathcal{O}_W$:

$$\Delta g_1^Z = g_1^Z - 1 = \frac{g^2 v^2}{8 c^2 \Lambda^2} f_W,$$
$$\Delta \kappa_\gamma = \kappa_\gamma - 1 = \frac{g^2 v^2}{8 \Lambda^2} (f_W + f_B),$$
$$\Delta \kappa_Z = \kappa_Z - 1 = \frac{g^2 v^2}{8 c^2 \Lambda^2} (c^2 f_W - s^2 f_B), \quad (29)$$
$$\lambda_\gamma = \lambda_Z = 0.$$

Therefore, we keep these two operators in our basis.

Now we can use the relations (24)–(26) to eliminate three of the four $\mathcal{O}_{WW}$, $\mathcal{O}_{BB}$, $\mathcal{O}_{\Phi,2}$, and $\mathcal{O}_{\Phi,4}$ remaining dimension-six operators. At this point the choice is driven by simplicity in the Higgs analysis. Our choice is to remove from the list the operators $\mathcal{O}_{BB}$, $\mathcal{O}_{\Phi,2}$, and $\mathcal{O}_{\Phi,4}$. This choice avoids the need of renormalization of the Higgs wave function Eq. (8) which affects all Higgs couplings while keeping operators which gives rise to all possible Lorentz structures in Eq. (16). This choice also allows for clear separation of those operators affecting the Higgs-gauge boson couplings from those affecting the Higgs-fermion couplings and makes the analysis simpler. Therefore, our dimension-six operator basis is

$$\{\mathcal{O}_{GG}, \mathcal{O}_{BW}, \mathcal{O}_{WW}, \mathcal{O}_W, \mathcal{O}_B, \mathcal{O}_{\Phi,1}, \mathcal{O}_{f\Phi}, \mathcal{O}_{\Phi f}^{(1)}, \mathcal{O}_{\Phi f}^{(3)}\}. \quad (30)$$

Now we can easily take advantage of all available experimental information in order to reduce the number of relevant parameters in the analysis of the Higgs data.

(i) Taking into account that the Z couplings to fermions are in agreement with the SM at the per mil level [30], the coefficients of all operators that modify these couplings are so constrained that they will have no impact in the Higgs physics. Therefore, we will not consider the operators $(\mathcal{O}_{\Phi f}^{(1)}, \mathcal{O}_{\Phi f}^{(3)})$ in our analyses (see also Ref. [26] for a recent analysis of constraints on these operators).

(ii) The precision measurement of parameters S, T, U in Eq. (43) leads to strong bounds on the coefficients of $\mathcal{O}_{BW}$ and $\mathcal{O}_{\Phi,1}$, thus allowing us to neglect the contribution of these operators.

(iii) Limits on low-energy flavor-changing interactions impose strong bounds on off-diagonal Yukawa couplings [31–36]. There may still be sizeable flavor-changing effects in $\bar{\tau} e$ and $\bar{\tau} \mu$ [34,35] which are, however, not relevant to the present analysis. Consequently we also discard from our basis the off-diagonal part of $\mathcal{O}_{f\Phi}$.

(iv) Flavor diagonal $\mathcal{O}_{f\Phi}$ from first and second generation only affect the present Higgs data via their contribution to the Higgs-gluon-gluon and Higgs-γ-γ vertex at one loop. The loop form factors are very suppressed for light fermions and correspondingly their effect is totally negligible in the analysis. Consequently, we keep only the fermionic operators $\mathcal{O}_{e\Phi,33}$, $\mathcal{O}_{u\Phi,33}$, and $\mathcal{O}_{d\Phi,33}$.

(v) The tree-level information on $h t \bar{t}$ from associate production has very large errors. So quantitatively the effects of the parameter $f_{u\Phi,33}$ enter via its contribution to the one-loop Higgs couplings to photon pairs and gluon pairs. At present these contributions can be absorbed in the redefinition of the parameters f_g and f_{WW}; therefore, we set $f_{\text{top}} \equiv 0$. In the future, when a larger luminosity will be accumulated, it will be necessary to introduce f_{top} as one of the parameters in the fit.

In brief the effective Lagrangian that we use in our analyses is

$$\mathcal{L}_{\text{eff}} = -\frac{\alpha_s v}{8\pi} \frac{f_g}{\Lambda^2} \mathcal{O}_{GG} + \frac{f_{WW}}{\Lambda^2} \mathcal{O}_{WW} + \frac{f_W}{\Lambda^2} \mathcal{O}_W$$
$$+ \frac{f_B}{\Lambda^2} \mathcal{O}_B + \frac{f_{\text{bot}}}{\Lambda^2} \mathcal{O}_{d\Phi,33} + \frac{f_\tau}{\Lambda^2} \mathcal{O}_{e\Phi,33}. \quad (31)$$

Notice that with this choice of basis all of the dimension-six operators considered contribute to the Higgs-gauge boson and Higgs-fermion couplings at the tree level.

III. ANALYSIS FRAMEWORK

In order to obtain the present constraints on the coefficients of the operators (31) we perform a chi-square test using the available data on the signal strength (μ) from Tevatron, LHC at 7 TeV and LHC at 8 TeV for the channels presented in Tables I, II, and III. We will also combine in the chi-square the data coming from the most precise determination of triple electroweak gauge boson couplings as well as the constraints coming from electroweak precision data (EWPD).

In order to predict the expected signal strengths in the presence of the new operators we need to include their effect in the production channels, as well as in the decay

TABLE I. Results included in the analysis for the Higgs decay modes listed except for the $\gamma\gamma$ channels.

Channel	$\mu^{\exp}$	Comment
$p\bar{p} \to W^+W^-$	$0.32^{+1.13}_{-0.32}$	CDF and D0 [37]
$p\bar{p} \to b\bar{b}$	$1.56^{+0.72}_{-0.73}$	CDF and D0 [38]
$p\bar{p} \to \gamma\gamma$	$3.6^{+3.0}_{-2.5}$	CDF and D0 [37]
$pp \to \tau\bar{\tau}$	$0.7^{+0.7}_{-0.7}$	ATLAS @ 7 and 8 TeV [39]
$pp \to b\bar{b}$	$-2.7^{+1.56}_{-1.56}$	ATLAS @ 7 TeV [40]
$pp \to b\bar{b}$	$1.0^{+1.42}_{-1.42}$	ATLAS @ 8 TeV [40]
$pp \to ZZ^* \to \ell^+\ell^-\ell^+\ell^-$	$1.3^{+0.5}_{-0.4}$	ATLAS @ 7 and 8 TeV [41]
$pp \to WW^* \to \ell^+\nu\ell^-\bar{\nu}$	$0.5^{+0.6}_{-0.6}$	ATLAS @ 7 TeV [42]
$pp \to WW^* \to \ell^+\nu\ell^-\bar{\nu}$	$1.5^{+0.6}_{-0.6}$	ATLAS @ 8 TeV [43]
$pp \to \tau\bar{\tau}$	$1.0^{+0.875}_{-0.875}$	CMS @ 7 TeV [44]
$pp \to \tau\bar{\tau}$	$0.625^{+0.625}_{-0.625}$	CMS @ 8 TeV [44]
$pp \to b\bar{b}$	$1.3^{+0.7}_{-0.6}$	CMS @ 7 and 8 TeV [45]
$pp \to ZZ^* \to \ell^+\ell^-\ell^+\ell^-$	$0.8^{+0.35}_{-0.28}$	CMS @ 7 and 8 TeV [46]
$pp \to WW^* \to \ell^+\nu\ell^-\bar{\nu}$	$0.74^{+0.25}_{-0.25}$	CMS @ 7 and 8 TeV [47]

branching ratios. We follow the approach described in Ref. [9], which we briefly summarize here. Assuming that the K factor associated with higher order corrections is the same for the SM and new contributions we write

$$\sigma_Y^{\text{ano}} = \left.\frac{\sigma_Y^{\text{ano}}}{\sigma_Y^{\text{SM}}}\right|_{\text{tree}} \sigma_Y^{\text{SM}}\big|_{\text{soa}}, \qquad (32)$$

$$\Gamma^{\text{ano}}(h \to X) = \left.\frac{\Gamma^{\text{ano}}(h \to X)}{\Gamma^{\text{SM}}(h \to X)}\right|_{\text{tree}} \Gamma^{\text{SM}}(h \to X)\big|_{\text{soa}} \qquad (33)$$

TABLE II. $H \to \gamma\gamma$ results from ATLAS [48,49] included in our analysis.

Channel	$\mu^{\exp}$	
	7 TeV	8 TeV
Unconverted central, low p_{T_t}	$0.52^{+1.45}_{-1.40}$	$1.0^{+0.9}_{-0.9}$
Unconverted central, high p_{T_t}	$0.23^{+1.98}_{-1.98}$	$0.35^{+1.1}_{-1.1}$
Unconverted rest, low p_{T_t}	$2.56^{+1.69}_{-1.69}$	$2.85^{+1.2}_{-1.2}$
Unconverted rest, high p_{T_t}	$10.47^{+3.66}_{-3.72}$	$1.8^{+1.4}_{-1.4}$
Converted central, low p_{T_t}	$6.10^{+2.62}_{-2.62}$	$1.5^{+1.25}_{-1.25}$
Converted central, high p_{T_t}	$-4.36^{+1.80}_{-1.80}$	$1.0^{+1.55}_{-1.55}$
Converted rest, low p_{T_t}	$2.73^{+1.98}_{-1.98}$	$2.35^{+1.2}_{-1.2}$
Converted rest, high p_{T_t}	$-1.57^{+2.91}_{-2.91}$	$0.55^{+1.65}_{-1.65}$
Converted transition	$0.41^{+3.55}_{-3.66}$	$2.0^{+2.0}_{-2.0}$
2 jets/2 jets high mass	$2.73^{+1.92}_{-1.86}$	$2.0^{+1.1}_{-1.1}$
2 jets low mass	$\cdots$	$3.6^{+2.15}_{-2.15}$
Lepton tagged	$\cdots$	$1.2^{+2.4}_{-2.4}$

with the superscripts ano (SM) standing for the value of the observable considering the anomalous and SM interactions (pure SM contributions). The ratios of the anomalous and SM cross sections of the subprocess Y ($= gg$, VBF, VH or $t\bar{t}H$) and of the decay widths are evaluated at tree level, and they are multiplied by the value for the state-of-the-art SM calculations, $\sigma_Y^{\text{SM}}\big|_{\text{soa}}$ and $\Gamma^{\text{SM}}(h\to X)\big|_{\text{soa}}$, presented in Ref. [51]. We did not include in our analyses an eventual invisible decay of the Higgs [52,53]; therefore the total width is obtained by summing over the decays into the SM particles. The evaluation of the relevant tree-level cross sections was done using the package MadGraph5 [54] with the anomalous Higgs interactions introduced using FeynRules [55]. We also cross-checked our results using COMPHEP [56,57] and VBFNLO [58].

For any final state F listed in Tables I, II, and III, we can write the theoretical signal strength as

TABLE III. $H \to \gamma\gamma$ results from CMS [50] included in our analysis.

Channel	$\mu^{\exp}$	
	7 TeV	8 TeV
$pp \to \gamma\gamma$ untagged 3	$1.53^{+1.61}_{-1.61}$	$3.78^{+1.77}_{-1.77}$
$pp \to \gamma\gamma$ untagged 2	$0.73^{+1.15}_{-1.15}$	$0.95^{+1.15}_{-1.15}$
$pp \to \gamma\gamma$ untagged 1	$0.66^{+0.95}_{-0.95}$	$1.51^{+1.03}_{-1.03}$
$pp \to \gamma\gamma$ untagged 0	$3.15^{+1.82}_{-1.82}$	$1.46^{+1.24}_{-1.24}$
$pp \to \gamma\gamma jj$	$4.21^{+2.04}_{-2.04}$	Loose $-0.61^{+2.03}_{-2.03}$
		Tight $1.32^{+1.57}_{-1.57}$

$$\mu_F = \frac{\epsilon_{gg}^F \sigma_{gg}^{ano}(1 + \xi_g) + \epsilon_{VBF}^F \sigma_{VBF}^{ano} + \epsilon_{WH}^F \sigma_{WH}^{ano} + \epsilon_{ZH}^F \sigma_{ZH}^{ano} + \epsilon_{t\bar{t}H}^F \sigma_{t\bar{t}H}^{ano}}{\epsilon_{gg}^F \sigma_{gg}^{SM} + \epsilon_{VBF}^F \sigma_{VBF}^{SM} + \epsilon_{WH}^F \sigma_{WH}^{SM} + \epsilon_{ZH}^F \sigma_{ZH}^{SM} + \epsilon_{t\bar{t}H}^F \sigma_{t\bar{t}H}^{SM}} \otimes \frac{Br^{ano}[h \to F]}{Br^{SM}[h \to F]}, \tag{34}$$

where ξ_g is the pull associated with the gluon fusion cross section uncertainties [see Eq. (37)], and the branching ratios and the anomalous cross sections are evaluated using the prescriptions (32) and (33). The weight of the different channels to each final state is encoded in the parameters ϵ_X with $X = VBF$, gg, WH,ZH, and $t\bar{t}H$.

The search for Higgs decaying into $b\bar{b}$ pairs takes place through Higgs production in association with a W or a Z so in this case

$$\epsilon_{gg}^{b\bar{b}} = \epsilon_{VBF}^{b\bar{b}} = \epsilon_{t\bar{t}H}^{b\bar{b}} = 0, \qquad \epsilon_{WH}^{b\bar{b}} = \epsilon_{ZH}^{b\bar{b}} = 1. \tag{35}$$

The ATLAS and CMS analyses of the 7 (8) TeV data separate the $\gamma\gamma$ signal into different categories and the contribution of each production mechanism to a given category is presented in Table 6 of ATLAS Ref. [48], Table 1 of ATLAS Ref. [49], and Table II of CMS Ref. [50] and we summarized them in Tables IV and V.

With the exception of the above processes, all other channels $F = WW^*$, ZZ^*, $\bar{\tau}\tau$ are treated as inclusive,

$$\epsilon_{gg}^F = \epsilon_{VBF}^F = \epsilon_{t\bar{t}H}^F = \epsilon_{WH}^F = \epsilon_{ZH}^F = 1. \tag{36}$$

For some final states the available LHC 8 TeV data have been presented combined with the 7 TeV results. In this case we construct the expected theoretical signal strength as an average of the expected signal strengths for the center-of-mass energies of 7 and 8 TeV. We weight the contributions by the total number of events expected at each energy in the framework of the SM (see Ref. [9] for details).

With all the data described above we perform a χ^2 test assuming that the correlations between the different channels are negligible except for the theoretical uncertainties which are treated with the pull method [59,60] in order to account for their correlations. The largest theoretical uncertainties are associated with the gluon fusion subprocess and to account for these errors we introduce two pull factors, one for the Tevatron (ξ_T) and one for the LHC at 7 and 8 TeV (ξ_L). They modify the corresponding predictions as shown in Eq. (34). We consider that the errors associated with the pulls are $\sigma_T = 0.4$ and $\sigma_L = 0.15$.

TABLE IV. Weight of each production mechanism for the different $\gamma\gamma$ categories in the ATLAS analyses of the 7 TeV data (upper values) and 8 TeV (lower values). For the 8 TeV analysis two new exclusive categories enriched in vector boson associated production were added with the 2 jets low mass (lepton tagged) category being built to select hadronic (leptonic) decays of the associated vector boson.

Channel	ϵ_{gg}	ϵ_{VBF}	ϵ_{WH}	ϵ_{ZH}	$\epsilon_{t\bar{t}H}$
Unconverted central, low p_{T_t}	1.06	0.579	0.550	0.555	0.355
	1.06	0.601	0.448	0.509	0.343
Unconverted central, high p_{T_t}	0.760	2.27	3.03	3.16	4.26
	0.868	2.17	1.25	1.64	2.91
Unconverted rest, low p_{T_t}	1.06	0.564	0.612	0.610	0.355
	1.06	0.601	0.544	0.622	0.343
Unconverted rest, high p_{T_t}	0.748	2.33	3.30	3.38	3.19
	0.868	2.16	1.44	1.87	2.06
Converted central, low p_{T_t}	1.06	0.578	0.581	0.555	0.357
	1.06	0.601	0.448	0.509	0.343
Converted central, high p_{T_t}	0.761	2.21	3.06	3.16	4.43
	0.880	2.07	1.31	1.58	2.91
Converted rest, low p_{T_t}	1.06	0.549	0.612	0.610	0.355
	1.06	0.586	0.544	0.622	0.343
Converted rest, high p_{T_t}	0.747	2.31	3.36	3.27	3.19
	0.857	2.16	1.57	1.92	2.23
Converted transition	1.02	0.752	1.01	0.943	0.532
	1.03	0.801	0.736	0.848	0.514
2 jets/2 jets high mass	0.257	11.1	0.122	0.111	0.177
	0.354	9.76	0.096	0.113	0.171
2 jets low mass (only 8 TeV)	0.685	0.730	6.63	6.84	2.74
Lepton tagged (only 8 TeV)	0.037	0.057	20	8.94	30.8

TABLE V. Weight of each production mechanism for the different $\gamma\gamma$ categories in the CMS analyses of the 7 TeV data (upper values) and 8 TeV (lower values). $\epsilon_{VH} = \epsilon_{ZH} = \epsilon_{WH}$. For the $pp \to \gamma\gamma jj$ category the 8 TeV data were divided into two independent subsamples labeled as "loose" and "tight" according to the requirement on the minimum transverse momentum of the softer jet and the minimum dijet invariant mass.

Channel	ϵ_{gg}	ϵ_{VBF}	ϵ_{VH}	$\epsilon_{t\bar{t}H}$
$pp \to \gamma\gamma$ untagged 3	1.04	0.579	0.788	0
	1.05	0.572	0.818	0
$pp \to \gamma\gamma$ untagged 2	1.04	0.579	0.788	0
	1.05	0.572	0.613	0
$pp \to \gamma\gamma$ untagged 1	1.01	0.868	1.18	1.77
	1.01	0.858	1.23	1.71
$pp \to \gamma\gamma$ untagged 0	0.698	2.46	3.74	5.32
	0.777	1.72	3.27	6.85
$pp \to \gamma\gamma jj$	0.309	10.6	0.197	0
$pp \to \gamma\gamma jj$ loose	0.605	6.44	0.409	0
$pp \to \gamma\gamma jj$ tight	0.263	11.0	0	0

Schematically we can write

$$\chi^2 = \min_{\xi_{pull}} \sum_j \frac{(\mu_j - \mu_j^{exp})^2}{\sigma_j^2} + \sum_{pull} \left(\frac{\xi_{pull}}{\sigma_{pull}}\right)^2, \qquad (37)$$

where j stands for channels presented in Tables I, II, and III. We denote the theoretically expected signal as μ_j, the observed best fit values as μ_j^{exp}, and error $\sigma_j = \sqrt{\frac{(\sigma_j^+)^2 + (\sigma_j^-)^2}{2}}$.

One important approximation in our analyses is that we neglect the effects associated with the distortions of the kinematic distributions of the final states due to the Higgs anomalous couplings arising from their non-SM-like Lorentz structure. Thus we implicitly assume that the anomalous contributions have the same detection efficiencies as the SM Higgs. A full simulation of the Higgs anomalous operators taking advantage of their special kinematic features might increase the current sensitivity on the anomalous couplings and it could also allow for breaking degeneracies with those operators which only lead to an overall modification of the strength of the SM vertices (see also Ref. [61]). But at present there is not enough public information to perform such analysis outside of the experimental collaborations.

In the next section we will also combine the results of Higgs data from Tevatron and LHC with those from the most precise determination of the triple electroweak gauge boson couplings (28). For consistency with our multi-parameter analysis, we include the results of the two-dimensional analysis in Ref. [28] which was performed in terms of $\Delta\kappa_\gamma$ and Δg_1^Z with $\Delta\kappa_Z$, λ_γ, and λ_Z as determined by the relations in Eq. (29):

$$g_1^Z = 0.984^{+0.049}_{-0.049}, \qquad \kappa_\gamma = 1.004^{+0.024}_{-0.025} \qquad (38)$$

with a correlation factor $\rho = 0.11$.

Finally for simplicity we will account for the constraints from EWPD on the dimension-six operators in terms of their contribution to the S, T, U parameters as presented for example in Ref. [25]. We will not consider additional effects associated with the possible energy dependence of those corrections. In particular the one-loop contributions from $\mathcal{O}_B$, $\mathcal{O}_W$, and $\mathcal{O}_{WW}$ read[3]

$$
\begin{aligned}
\alpha\Delta S = \frac{1}{6}\frac{e^2}{16\pi^2}\bigg\{ &3(f_W + f_B)\frac{m_H^2}{\Lambda^2}\log\left(\frac{\Lambda^2}{m_H^2}\right) \\
&+ 2[(5c^2 - 2)f_W - (5c^2 - 3)f_B]\frac{m_Z^2}{\Lambda^2}\log\left(\frac{\Lambda^2}{m_H^2}\right) \\
&- [(22c^2 - 1)f_W - (30c^2 + 1)f_B]\frac{m_Z^2}{\Lambda^2}\log\left(\frac{\Lambda^2}{m_Z^2}\right) \\
&- 24c^2 f_{WW}\frac{m_Z^2}{\Lambda^2}\log\left(\frac{\Lambda^2}{m_H^2}\right)\bigg\},
\end{aligned}
\qquad (39)
$$

$$
\begin{aligned}
\alpha\Delta T = \frac{3}{4c^2}\frac{e^2}{16\pi^2}\bigg\{ &f_B\frac{m_H^2}{\Lambda^2}\log\left(\frac{\Lambda^2}{m_H^2}\right) + (c^2 f_W + f_B)\frac{m_Z^2}{\Lambda^2} \\
&\times\log\left(\frac{\Lambda^2}{m_H^2}\right) + [2c^2 f_W + (3c^2 - 1)f_B]\frac{m_Z^2}{\Lambda^2}\log\left(\frac{\Lambda^2}{m_Z^2}\right)\bigg\},
\end{aligned}
\qquad (40)
$$

$$
\begin{aligned}
\alpha\Delta U = -\frac{1}{3}\frac{e^2 s^2}{16\pi^2}\bigg\{ &(-4f_W + 5f_B)\frac{m_Z^2}{\Lambda^2}\log\left(\frac{\Lambda^2}{m_H^2}\right) \\
&+ (2f_W - 5f_B)\frac{m_Z^2}{\Lambda^2}\log\left(\frac{\Lambda^2}{m_Z^2}\right)\bigg\}.
\end{aligned}
\qquad (41)
$$

At present the most precise determination of S, T, U from a global fit to EWPD yields the following values and correlation matrix:

$$\Delta S = 0.00 \pm 0.10, \quad \Delta T = 0.02 \pm 0.11, \quad \Delta U = 0.03 \pm 0.09, \qquad (42)$$

$$\rho = \begin{pmatrix} 1 & 0.89 & -0.55 \\ 0.89 & 1 & -0.8 \\ -0.55 & -0.8 & 1 \end{pmatrix}. \qquad (43)$$

IV. PRESENT STATUS

Initially let us focus on the scenario where the Higgs couplings to fermions assume their SM values; i.e.,

---

[3]Should we have chosen a basis with $\mathcal{O}_{\Phi,2}$ and/or $\mathcal{O}_{\Phi,4}$, the corresponding contributions would read $\alpha\Delta S = -\frac{8}{9}\alpha\Delta T = \frac{1}{6}\frac{e^2}{16\pi^2}(f_{\Phi,2} - f_{\Phi,4})\frac{v^2}{\Lambda^2}\log(\frac{\Lambda^2}{m_H^2})$.

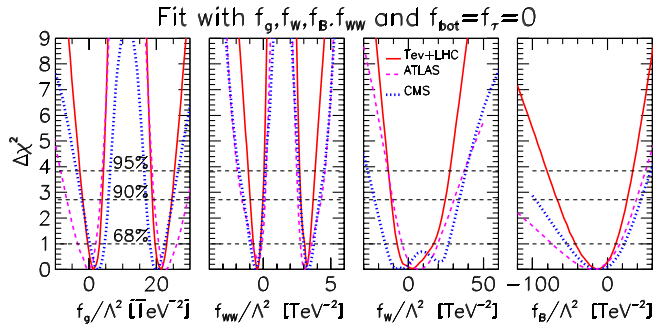FIG. 1 (color online). $\Delta\chi^2$ as a function of f_g, f_{WW}, f_W, and f_B for $f_{\rm bot} = f_\tau = 0$. Each panel contains three lines: the dashed (dotted) line was obtained using only the ATLAS (CMS) data while the solid line stands for the result using all the available data from ATLAS, CMS, and Tevatron. In each panel $\Delta\chi^2$ is marginalized over the three undisplayed parameters.

we set $f_{\rm bot} = f_\tau = 0$ and fit the available data using $\{f_g, f_W, f_B, f_{WW}\}$ as free independent parameters.[4] Figure 1 displays the $\Delta\chi^2$ as a function of the four free parameters after marginalizing over the three undisplayed ones. We present the results using only ATLAS data, only CMS data, and combining all data from ATLAS, CMS, and the Tevatron collaborations; see figure for the conventions. As we can see, the $\Delta\chi^2$ as a function of f_g exhibits two degenerate minima in all cases due to the interference between SM and anomalous contributions. The gluon fusion Higgs production cross section is too depleted for f_g values between the minima. In the case of the chi-square dependence upon f_{WW} there is also an interference between anomalous and SM contributions; however, the degeneracy of the minima is lifted since the f_{WW} coupling contributes to Higgs decay into photons, but also to its decay into WW^* and ZZ^* as well as in Vh associated and vector boson fusion production mechanisms. Furthermore, just looking at the scales, we can see that f_{WW} is better determined by the Higgs data than f_B or f_W. This is expected since the former coupling modifies the Higgs decay into two photons, which is a one-loop process in the SM, and that is presently the main Higgs detection mode. In general the ATLAS, CMS, and combined data lead to similar chi-square behavior with respect to the fitting parameters; however, there are small differences between the ATLAS and CMS results for f_g and f_{WW}. Altogether we find $\chi^2_{\rm min} = 44.4$ for the combined analysis and the SM lies at $\chi^2_{\rm SM} = 49.4$, i.e., within the 71% C.L. region in the four-dimensional parameter space. That is, the SM is in agreement with the ATLAS, CMS, and Tevatron results at better than 1.05σ level.

We translate the results displayed in Fig. 1 in terms of physical observables in Fig. 2, which shows the $\Delta\chi^2$

[4]This scenario is a straightforward generalization of the first scenario discussed in Ref. [9].
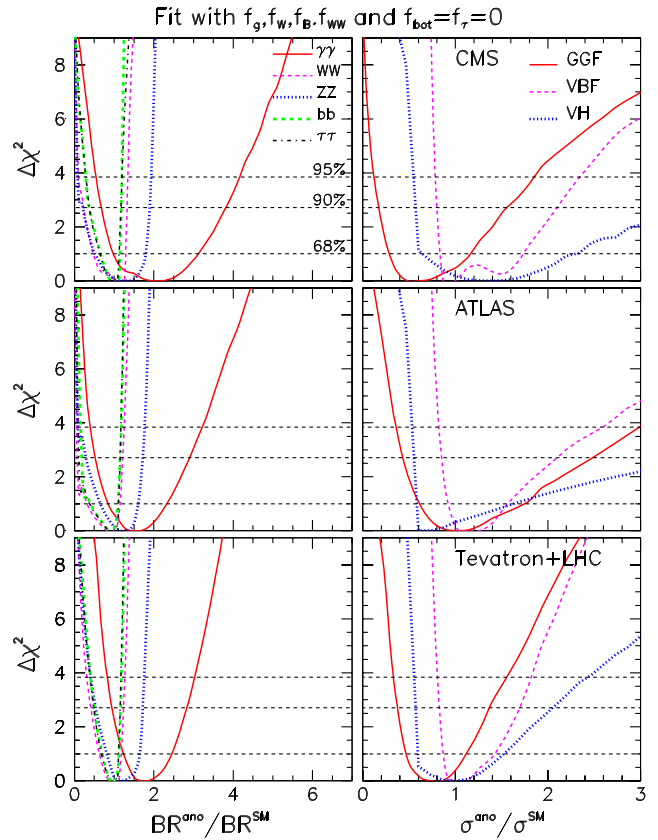

FIG. 2 (color online). The left (right) panels contain the chi-square dependence with the Higgs branching ratios (Higgs production cross sections) normalized to the SM values. The top (middle) [bottom] panels were obtained using the CMS (ATLAS) [combined ATLAS, CMS, and Tevatron] data. The dependence of $\Delta\chi^2$ on the branching ratio to the fermions shows the effect of the other parameters in the total decay width.

dependence on the Higgs decay branching ratios and production cross sections. Comparing the top and middle panels we can see that there is a small difference between ATLAS and CMS results for the Higgs branching ratio into two photons since the CMS result prefers larger values, though at present both best fit values lie within less than 1σ. Analogously for the gluon fusion Higgs production cross section CMS results slightly prefer smaller values. Examining the combined data sets we see that there is a slight preference for an enhanced Higgs branching ratio into two photons and a depleted gluon fusion cross section; however, as mentioned above the results are compatible with the SM predictions at better than 71% C.L.

The effect of combining the Higgs data with the triple gauge vertex (TGV) data and the EWPD is displayed in Fig. 3; see the first column for analysis with SM fermion couplings. When including EWPD we assumed a scale of 10 TeV in the evaluation of the logarithms in Eqs. (39)–(41). Since f_B and f_W are the only fit parameters
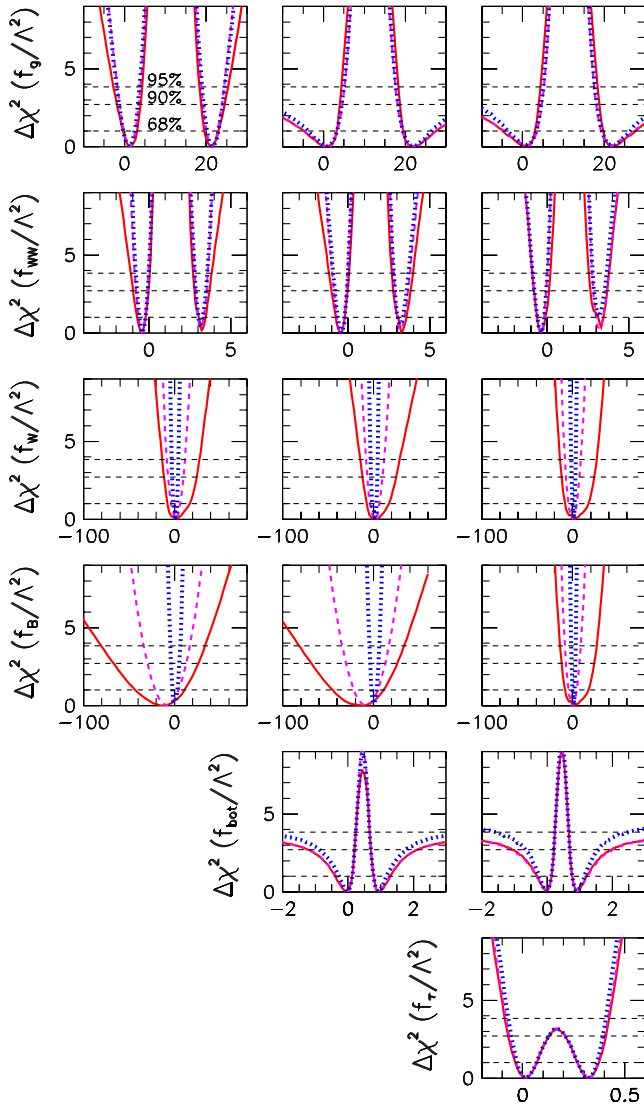
FIG. 3 (color online). $\Delta\chi^2$ dependence on the fit parameters when we consider all collider (ATLAS, CMS, and Tevatron) data (solid red line), collider and TGV data (dashed purple line), and collider, TGV, and EWPD (dotted blue line) using $\Lambda = 10^4$ GeV. The rows depict the $\Delta\chi^2$ dependence with respect to the fit parameter shown on the left of the row. In the first column we use f_g, f_{WW}, f_W, and f_B as fitting parameters with $f_{bot} = f_\tau = 0$. In the second column the fitting parameters are f_g, f_{WW}, f_W, f_B, and f_{bot} with $f_\tau = 0$. In panels on the right column we fit the data in terms of f_g, f_{WW}, $f_W = f_B$, f_{bot}, and f_τ.

columns in Table VI.[5] Inclusion of the TGV data has no quantitative impact on the values of χ^2_{min} or the SM C.L. Adding the EWPD increases $\Delta\chi^2_{min,(SM)}$ to 45.1 (51.3) so the SM lies in the full combined analysis at the 82% C.L. four-dimensional region in agreement with these combined results at 1.3σ level.

With respect to correlations between the allowed ranges of parameters the strongest correlations appear between f_g and f_{WW} and we illustrate them in the left panel of Fig. 4, which contains the 68%, 90%, 95%, and 99% C.L. two-dimensional projection in the plane $f_g \times f_{WW}$ of the four-dimensional allowed regions after marginalization over the undisplayed parameters. The results are shown for the combination of ATLAS, CMS, Tevatron, and TGV data sets.[6] As we can see, this panel exhibits four isolated islands that originate from the interference between anomalous and SM contributions in $H\gamma\gamma$ and Hgg vertices. Within each island there is a strong anticorrelation between f_g and f_{WW} that stems from the data on Higgs to two photons as discussed in Ref. [9].

Since the physics described by the four allowed regions in the left panel of Fig. 4 is the same, i.e., the rate of $\gamma\gamma$ events, they can be translated into correlations between the Higgs branching ratio into photons and its gluon fusion production cross section as depicted in the left panel of Fig. 5. Clearly, these quantities are anticorrelated since their product is the major source of Higgs events decaying into two photons.

Let us now turn to the effects of allowing for modifications of the Higgs couplings to fermions. We first do so by augmenting the set of parameters by the anomalous bottom Yukawa coupling f_{bot}; i.e., our free parameters are $\{f_g, f_W, f_B, f_{WW}, f_{bot}\}$, where we are still keeping $f_\tau = 0$. We present in the middle panels of Fig. 3 the chi-square as a function of the fitting parameters in this case. Comparing with the first column of panels in this figure we see the allowed range for f_g becomes much larger and the one for f_{bot} is also large. This behavior emanates from the fact that at large f_{bot} the Higgs branching ratio into b-quark pairs approaches 1, so to fit the data for any channel $F \neq bb$, the gluon fusion cross section must be enhanced in order to compensate the dilution of the $H \to F$ branching ratios. This is clearly shown in Fig. 6, which depicts the strong correlation between the allowed values of $f_g \times f_{bot}$.

that modify the triple gauge vertices at tree level, they are the ones that show the largest impact of the TGV data, especially f_B. Moreover, f_B and f_W are also the parameters that more strongly feel the inclusion of the EWPD; see Eqs. (39)–(41). In brief, the largest impact of the TGV and EWPD is on f_W and f_B with a marginal effect on f_g and f_{WW}. The best fit values and 90% C.L. allowed ranges for the couplings and observables in the combined analysis of Tevatron + LHC + TGV data can be found in the two first

---

[5]Assuming that the top is the only particle contributing in the loop of the Higgs to gluons vertex with a non-negligible form factor, the best fit points and 90% C.L. ranges for f_g could be directly translated to values for f_{top} as $f_{top}^{best} = 1.9$, 31 and $[-1.7, 5] \cup [27, 35]$ at 90% C.L. for the analysis with SM fermion couplings and $f_{top}^{best} = 1.9$, 31 and $[-30, 6.9] \cup [26, 63]$ at 90% C.L. for the analysis with f_{bot} and f_τ.

[6]Here we do not include EWPD to avoid the introduction of a model-dependent scale needed to evaluate the logarithms present in Eqs. (39)–(41).

TABLE VI.   Best fit values and 90% C.L. allowed ranges for the combination of all available Tevatron and LHC Higgs data as well as TGV.

| | Fit with $f_{bot} = f_\tau = 0$ | | Fit with f_{bot} and f_τ | |
	Best fit	90% C.L. allowed range	Best fit	90% C.L. allowed range
f_g/Λ^2 (TeV^{-2})	1.3, 21.4	$[-1.2, 3.5] \cup [19, 24]$	1.3, 21.4	$[-21, 4.8] \cup [18, 44]$
f_{WW}/Λ^2 (TeV^{-2})	-0.43	$[-0.80, -0.10] \cup [2.85, 3.55]$	-0.39	$[-0.80, 0] \cup [2.85, 3.65]$
f_W/Λ^2 (TeV^{-2})	1.43	$[-7.0, 10]$	0.42	$[-7.4, 7.6]$
f_B/Λ^2 (TeV^{-2})	-8.4	$[-30, 13]$	0.42	$[-7.4, 7.6]$
f_{bot}/Λ^2 (TeV^{-2})	$\cdots$	$\cdots$	0.00, 0.90	$[-1.2, 0.20] \cup [0.70, 2.1]$
f_τ/Λ^2 (TeV^{-2})	$\cdots$	$\cdots$	0.02, 0.32	$[-0.07, 0.13] \cup [0.2, 0.40]$
$BR_{\gamma\gamma}^{ano}/BR_{\gamma\gamma}^{SM}$	1.75	$[1.15, 2.62]$	1.70	$[0.20, 3.00]$
$BR_{WW}^{ano}/BR_{WW}^{SM}$	0.97	$[0.75, 1.14]$	1.02	$[0.11, 1.94]$
$BR_{ZZ}^{ano}/BR_{ZZ}^{SM}$	1.13	$[0.78, 1.45]$	1.03	$[0.11, 1.96]$
$BR_{bb}^{ano}/BR_{bb}^{SM}$	1.01	$[0.84, 1.06]$	1.04	$[0.53, 1.53]$
$BR_{\tau\tau}^{ano}/BR_{\tau\tau}^{SM}$	1.01	$[0.84, 1.06]$	0.85	$[0.05, 2.25]$
$\sigma_{gg}^{ano}/\sigma_{gg}^{SM}$	0.79	$[0.47, 1.23]$	0.79	$[0.35, 8]$
$\sigma_{VBF}^{ano}/\sigma_{VBF}^{SM}$	1.02	$[0.92, 1.21]$	1.00	$[0.91, 1.13]$
$\sigma_{VH}^{ano}/\sigma_{VH}^{SM}$	0.98	$[0.58, 1.40]$	1.02	$[0.57, 1.49]$

On the other hand, allowing for $f_{bot} \neq 0$ has a small impact on the parameters affecting the Higgs couplings to electroweak gauge bosons f_W, f_B, and f_{WW} as seen by comparing the corresponding left and central panels of Fig. 3, even prior to the inclusion of TGV constraints on f_W and f_B. See also the right panel of Fig. 4 from where we learn that the four allowed regions do now extend to much larger values of f_g while not so much for f_{WW}. This is due to the independent information from the $b\bar{b}$ channel on the associated production cross section and from $\gamma\gamma$ results; see Fig. 7. This last one is also illustrated in the right panel of Fig. 5, which shows that the gluon fusion production

cross section can now be much larger than the SM one but only as long as the Higgs branching ratio into photons is below the SM value in order to fit the observed rate of $\gamma\gamma$ events.

The effect of f_{bot} can also be understood by comparing the upper and central lines in Fig. 7 which contain the chi-square dependence on Higgs branching ratios (left) and production cross sections (right) for the analysis with $f_{bot} = 0$ (upper) and $f_{bot} \neq 0$ (central). We can immediately see that the bounds on branching ratios and cross sections get loosened, with the VBF and VH production cross sections being the least affected quantities.
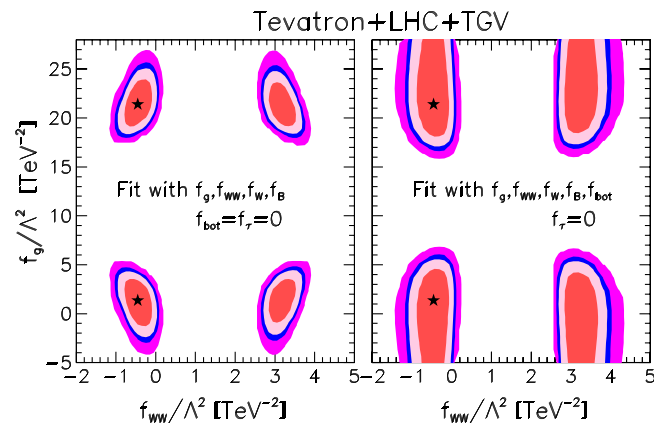

FIG. 4 (color online).   In the left (right) panel we present the 68%, 90%, 95%, and 99% C.L. allowed regions in the plane $f_g \times f_{WW}$ when we fit the ATLAS, CMS, Tevatron, and TGV data varying f_g, f_{WW}, f_W, and f_B (f_g, f_{WW}, f_W, f_B, and f_{bot}). The stars stand for the global minima and we marginalized over the undisplayed parameters.
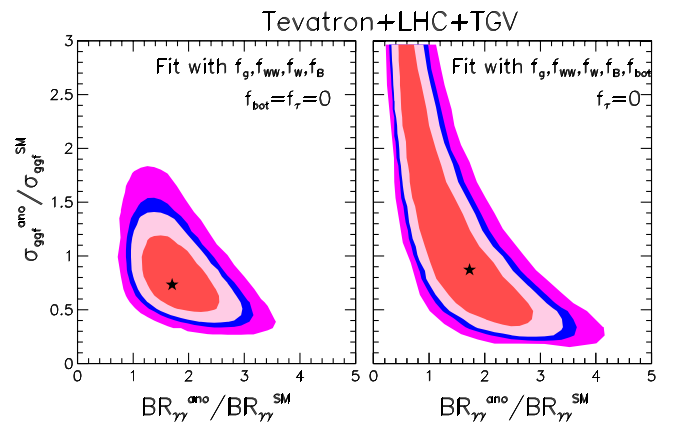

FIG. 5 (color online).   In the left (right) panel we present the 68%, 90%, 95%, and 99% C.L. allowed regions in the plane $\sigma_{gg}^{ano}/\sigma_{gg}^{SM} \times Br(h \to \gamma\gamma)^{ano}/Br(h \to \gamma\gamma)^{SM}$ when we fit the ATLAS, CMS, Tevatron, and TGV data varying f_g, f_{WW}, f_W, and f_B (f_g, f_{WW}, f_W, f_B, and f_{bot}). The stars stand for the global minima and we marginalized over the undisplayed parameters.
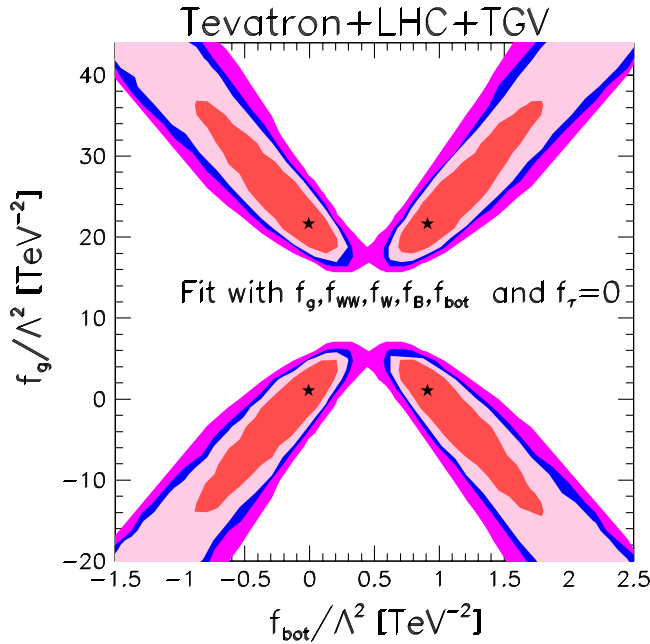
FIG. 6 (color online). We present the 68%, 90%, 95%, and 99% C.L. allowed regions in the plane $f_{\rm bot} \times f_g$ when we fit the ATLAS, CMS, Tevatron, and TGV data varying f_g, f_{WW}, f_W, f_B, and $f_{\rm bot}$. The stars stand for the global minima and we have marginalized over the undisplayed parameters.

Furthermore, the gluon fusion cross section becomes unbound from above already at 95% C.L. The reason for this deterioration of the constraints is due to the strong correlation between f_g and $f_{\rm bot}$ we just mentioned.

The impact of $f_{\rm bot}$ on the fits is due to the absence of data on the direct process $pp \to h \to b\bar{b}$ due to the huge SM backgrounds. One way to mitigate the lack of information on this channel is to have smaller statistical errors in the processes taking place via VBF or VH associated production. However, this will require a larger data sample than that which is presently available.

Finally we study the effect of allowing the τ Yukawa coupling to deviate from its SM value as well. For the sake of simplicity we keep the number of free parameters equal to five and we choose them to be $\{f_g, f_{WW}, f_W = f_B, f_{\rm bot}, f_\tau\}$. We present in the right panels of Fig. 3 the chi-square as a function of the free parameters in this case and in the lower panels in Fig. 7 the corresponding dependence for the decay branching ratios and production cross sections. The results are that the inclusion of f_τ in the analysis does not introduce any further strong correlation and that the determination of the other parameters is not affected very much. This is so because the data on $pp \to h \to \tau^+\tau^-$ cuts off any strong correlation between f_τ and f_g. The corresponding best fit values and allowed 90% C.L. ranges for the parameters and observables are given in the right two columns in Table VI. We see that at the best fit point the present global analysis favors a
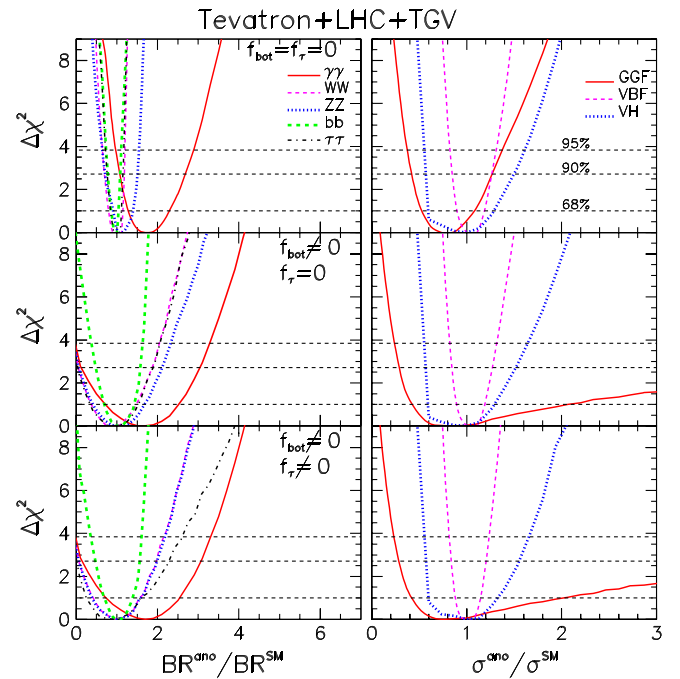

FIG. 7 (color online). Chi-square dependence upon Higgs branching ratios (left panels) and production cross sections (right panels) when we consider all collider (ATLAS, CMS, and Tevatron) and TGV data. In the upper panels we used f_g, f_{WW}, f_W, and f_B as fitting parameters with $f_{\rm bot} = f_\tau = 0$, while in the middle panels the fitting parameters are f_g, f_{WW}, f_W, f_B, and $f_{\rm bot}$ with $f_\tau = 0$. In the lower row we parametrize the data in terms of f_g, f_{WW}, $f_W = f_B$, $f_{\rm bot}$, and f_τ. The dependence of $\Delta\chi^2$ on the branching ratio to the fermions not considered in the analysis arises from the effect of the other parameters in the total decay width.

$BR_{\tau\tau}^{\rm ano}/BR_{\tau\tau}^{\rm SM}$ smaller than 1 (0.85) which leads to two possible values of f_τ: one small positive correction to the negative SM Yukawa coupling and one larger positive which will flip the sign of the H$\tau\tau$ coupling but give the same absolute value. This is the origin of the two minima observed in the lowest panel in Fig. 3. Also, the inclusion of the fermion couplings has no impact on the values of $\chi^2_{\rm min,(SM)}$. Thus the corresponding C.L. of the SM is only affected because we have now one extra free parameter in the analysis and it still holds that the SM is in overall agreement with the Higgs and TGV results at better than 1σ level.

V. DISCUSSIONS AND CONCLUSIONS

As the ATLAS and CMS experiments accumulate more and more luminosity we start to better probe the couplings of the recently discovered Higgs-like state. In this work we used a bottom-up approach to describe departures of the Higgs couplings from the SM predictions. In a model-independent framework these effects can be parametrized

in terms of an effective Lagrangian. Assuming that the observed state is a member of an $SU(2)_L$ doublet, and therefore the $SU(2)_L \times U(1)_Y$ gauge symmetry is linearly realized, they appear at lowest order as dimension-six operators with unknown coefficients containing all the SM fields including the light scalar doublet; for details return to Sec. II where we give the full list of operators affecting the Higgs couplings to gauge bosons and fermions. Not all the operators in Eqs. (2) and (17) are independent because at any order they are related by the equations of motion. This allows for a ''freedom of choice'' in the election of the basis of operators to be used in the analysis.

We have argued in Sec. II C that in the absence of any *a priori* knowledge on the form of the new physics the most sensible choice of basis should contain operators whose coefficients are more easily related to existing data from other well tested sectors of the theory, i.e., not only the LHC data on the Higgs production, but also EWPD and searches for anomalous triple gauge vertices. In this approach we reduce the operator basis to the six operators in Eq. (31) which are directly testable with an analysis of the existing Higgs data. The summary of our present determination of Higgs couplings, production cross sections, and decay branching ratios from the analysis of the Higgs and TGV data can be found in Table VI. Here, we present the results for new physics scenarios with SM (two left columns) and nonstandard (two right columns) Higgs couplings to fermions.

Generically in any analysis, we obtained that the SM predictions for each individual coupling and observable are within the corresponding 90% C.L. range with the only exception being the Higgs branching ratio into two photons for the analysis with SM couplings to fermions. Still at the best fit, the present analyses prefer a larger-than-SM branching ratio to photons and a smaller-than-SM gluon fusion production cross section and decay branching ratio into τ's.

Should these results be confirmed they might be an indirect signal for physics beyond the standard model that is showing in the right place, i.e., an observable for which the SM contributions occur only at the one-loop level. This allows for small new physics contributions to these observable to be observed easily. For instance, there has been a great interest in processes that can modify the Higgs branching ratio into two photons [62].

The presence of nonvanishing coefficients for the dimension-six operators alters the high-energy behavior of the scattering amplitudes of SM particles. The scale where unitarity is violated at tree level in a given process can be used as a rough estimation for the onset of new physics. For instance, the $2 \rightarrow 2$ scattering of SM (Higgs or gauge) bosons has been used to test the validity of a theory containing dimension-six effective operators [63,64]. The operators O_W and O_B give rise to a contribution to the neutral $W_L^- W_L^+$, $Z_L Z_L$, and HH channels which grows like $(f_{W,B} s / M_W^2)^2$ [63]. Taking the best fit values for the anomalous parameters obtained in our fits, a very strong hypothesis, the study of unitarity violation indicates that the scale of new physics beyond SM is of the order of 5–10 TeV. Certainly, this number should be taken with a grain (not to say a lot) of salt. Nevertheless we expect, as the errors shrink with larger data sets, that the 68% C.L. allowed regions can be used to set limits to the new physics scale in a not so far future.

ACKNOWLEDGMENTS

[1] F. Englert and R. Brout, Phys. Rev. Lett. **13,** 321 (1964).

[2] P. W. Higgs, Phys. Rev. Lett. **13,** 508 (1964).

[3] P. W. Higgs, Phys. Lett. **12,** 132 (1964).

[4] G. Guralnik, C. Hagen, and T. Kibble, Phys. Rev. Lett. **13,** 585 (1964).

[5] P. W. Higgs, Phys. Rev. **145,** 1156 (1966).

[6] T. Kibble, Phys. Rev. **155,** 1554 (1967).

[7] CMS Collaboration, Phys. Lett. B **716,** 30 (2012); ATLAS Collaboration, Phys. Lett. B **716,** 1 (2012).

[8] A partial list of works includes S. Y. Choi, D. J. Miller, M. M. Muhlleitner, and P. M. Zerwas, Phys. Lett. B **553,** 61 (2003); K. Odagiri, J. High Energy Phys. 03 (2003) 009; C. P. Buszello, I. Fleck, P. Marquard, and J. J. van der Bij, Eur. Phys. J. C **32,** 209 (2004); C. P. Buszello and P. Marquard, arXiv:hep-ph/0603209; A. Bredenstein, A. Denner, S. Dittmaier, and M. M. Weber, Phys. Rev. D **74,** 013004 (2006); P. S. Bhupal Dev, A. Djouadi, R. M. Godbole, M. M. Muhlleitner, and S. D. Rindani, Phys. Rev. Lett. **100,** 051801 (2008); R. M. Godbole, D. J.

Miller, and M. M. Muhlleitner, J. High Energy Phys. 12 (2007) 031; K. Hagiwara, Q. Li, and K. Mawatari, J. High Energy Phys. 07 (2009) 101; C. Englert, C. Hackstein, and M. Spannowsky, Phys. Rev. D **82**, 114024 (2010); U. De Sanctis, M. Fabbrichesi, and A. Tonero, Phys. Rev. D **84**, 015013 (2011); V. Barger and P. Huang, Phys. Rev. D **84**, 093001 (2011); S. Bolognesi, Y. Gao, A. V. Gritsan, K. Melnikov, M. Schulze, N. V. Tran, and A. Whitbeck, Phys. Rev. D **86**, 095031 (2012); J. Ellis, D. S. Hwang, V. Sanz, and T. You, arXiv:1208.6002; P. Avery *et al.*, arXiv:1210.0896; R. Boughezal, T. J. LeCompte, and F. Petriello, arXiv:1208.4311; D. Stolarski and R. Vega-Morales, Phys. Rev. D **86**, 117504 (2012); S. Y. Choi, M. M. Muhlleitner, and P. M. Zerwas, arXiv:1209.5268; A. Alves, Phys. Rev. D **86**, 113010 (2012); J. Ellis, R. Fok, D. S. Hwang, V. Sanz, and T. You, arXiv:1210.5229; J. Ellis, V. Sanz, and T. You, arXiv:1211.3068.

[9] T. Corbett, O. J. P. Eboli, J. Gonzalez-Fraile, and M. C. Gonzalez-Garcia, Phys. Rev. D **86**, 075013 (2012).

[10] For other postdiscovery analyses of the *X* particle couplings, see also J. Ellis and T. You, J. High Energy Phys. 09 (2012) 123; I. Low, J. Lykken, and G. Shaughnessy, Phys. Rev. D **86**, 093012 (2012); P. P. Giardino, K. Kannike, M. Raidal, and A. Strumia, Phys. Lett. B **718**, 469 (2012); M. Montull and F. Riva, J. High Energy Phys. 11 (2012) 018; J. R. Espinosa, C. Grojean, M. Muhlleitner, and M. Trott, J. High Energy Phys. 12 (2012) 045; D. Carmi, A. Falkowski, E. Kuflik, T. Volansky, and J. Zupan, J. High Energy Phys. 10 (2012) 196; S. Banerjee, S. Mukhopadhyay, and B. Mukhopadhyaya, J. High Energy Phys. 10 (2012) 062; F. Bonner, T. Ota, M. Rauch, and W. Winter, Phys. Rev. D **86**, 093014 (2012); T. Plehn and M. Rauch, Europhys. Lett. **100**, 11002 (2012); A. Djouadi, arXiv:1208.3436; B. Batell, S. Gori, and L. T. Wang, arXiv:1209.6832; G. Cacciapaglia, A. Deandrea, G. D. La Rochelle, and J.-B. Flament, arXiv:1210.8120; G. Moreau, arXiv:1210.3977.

[11] S. Weinberg, Physica (Amsterdam) **96**, 327 (1979); see also H. Georgi, *Weak Interactions and Modern Particle Theory* (Benjamim/Cummings, Menlo Park, 1984); J. F. Donoghue, E. Golowich, and B. R. Holstein, *Dynamics of the Standard Model* (Cambridge University Press, Cambridge, England, 1992).

[12] W. Buchmuller and D. Wyler, Nucl. Phys. **B268**, 621 (1986).

[13] C. N. Leung, S. Love, and S. Rao, Z. Phys. C **31**, 433 (1986).

[14] A. De Rujula, M. Gavela, P. Hernandez, and E. Masso, Nucl. Phys. **B384**, 3 (1992).

[15] K. Hagiwara, S. Ishihara, R. Szalapski, and D. Zeppenfeld, Phys. Rev. D **48**, 2182 (1993).

[16] K. Hagiwara, R. Szalapski, and D. Zeppenfeld, Phys. Lett. B **318**, 155 (1993).

[17] K. Hagiwara, S. Matsumoto, and R. Szalapski, Phys. Lett. B **357**, 411 (1995).

[18] M. Gonzalez-Garcia, Int. J. Mod. Phys. A **14**, 3121 (1999); F. de Campos, M. C. Gonzalez-Garcia, and S. F. Novaes, Phys. Rev. Lett. **79**, 5210 (1997); M. C. Gonzalez-Garcia, S. M. Lietti, and S. F. Novaes, Phys. Rev. D **57**, 7045 (1998); O. J. P. Eboli, M. C. Gonzalez-Garcia, S. M. Lietti, and S. F. Novaes, Phys. Lett. B **434**, 340 (1998);

M. C. Gonzalez-Garcia, S. M. Lietti, and S. F. Novaes, Phys. Rev. D **59**, 075008 (1999); O. J. P. Eboli, M. C. Gonzalez-Garcia, S. M. Lietti, and S. F. Novaes, Phys. Lett. B **478**, 199 (2000).

[19] G. Passarino, arXiv:1209.5538.

[20] B. Grzadkowski, M. Iskrzynski, M. Misiak, and J. Rosiek, J. High Energy Phys. 10 (2010) 085.

[21] F. Bonnet, M. Gavela, T. Ota, and W. Winter, Phys. Rev. D **85**, 035016 (2012).

[22] H. D. Politzer, Nucl. Phys. **B172**, 349 (1980); H. Georgi, Nucl. Phys. **B361**, 339 (1991); C. Arzt, Phys. Lett. B **342**, 189 (1995); H. Simma, Z. Phys. C **61**, 67 (1994).

[23] J. Wudka, Int. J. Mod. Phys. A **09**, 2301 (1994).

[24] C. Arzt, M. B. Einhorn, and J. Wudka, Nucl. Phys. **B433**, 41 (1995).

[25] S. Alam, S. Dawson, and R. Szalapski, Phys. Rev. D **57**, 1577 (1998).

[26] F. del Aguila and J. de Blas, Fortschr. Phys. **59**, 1036 (2011); F. del Aguila, J. de Blas, and M. Perez-Victoria, Phys. Rev. D **78**, 013010 (2008).

[27] K. Hagiwara, R. Peccei, D. Zeppenfeld, and K. Hikasa, Nucl. Phys. **B282**, 253 (1987).

[28] LEP Collaborations and LEP TGC Working Group, Report No. LEPEWWG/TGC/2003-01.

[29] K. Nakamura *et al.* (Particle Data Group), J. Phys. G **37**, 075021 (2010).

[30] ALEPH Collaboration, CDF Collaboration, D0 Collaboration, DELPHI Collaboration, L3 Collaboration, OPAL Collaboration, SLD Collaboration, LEP Electroweak Working Group, Tevatron Electroweak Working Group, and SLD Electroweak Heavy Flavour Groups, arXiv:1012.2367.

[31] S. Kanemura, T. Ota, and K. Tsumura, Phys. Rev. D **73**, 016006 (2006).

[32] P. Paradisi, J. High Energy Phys. 02 (2006) 050.

[33] E. Gabrielli and B. Mele, Phys. Rev. D **83**, 073009 (2011).

[34] S. Davidson and G. J. Grenier, Phys. Rev. D **81**, 095016 (2010); S. Davidson and P. Verdier, arXiv:1211.1248.

[35] A. Goudelis, O. Lebedev, and J.-h. Park, Phys. Lett. B **707**, 369 (2012).

[36] G. Blankenburg, J. Ellis, and G. Isidori, Phys. Lett. B **712**, 386 (2012).

[37] The CDF Collaboration, the D0 Collaboration, the Tevatron New Physics, and Higgs Working Group, arXiv:1207.0449.

[38] CDF and D0 Collaborations, http://kds.kek.jp/conference Display.py?confId=10808.

[39] ATLAS Collaboration, http://kds.kek.jp/conferenceDisplay. py?confId=10808.

[40] ATLAS Collaboration, http://kds.kek.jp/conferenceDisplay .py?confId=10808.

[41] ATLAS Collaboration, Report No. ATLAS-CONF-2012-169.

[42] ATLAS Collaboration, Phys. Rev. D **86**, 032003 (2012).

[43] ATLAS Collaboration, http://kds.kek.jp/conferenceDisplay. py?confId=10808.

[44] CMS Collaboration, http://kds.kek.jp/conferenceDisplay.py? confId=10808.

[45] CMS Collaboration, http://kds.kek.jp/conferenceDisplay.py? confId=10808.

[46] CMS Collaboration, http://kds.kek.jp/conferenceDisplay.py? confId=10808.

[47] CMS Collaboration, http://kds.kek.jp/conferenceDisplay.py?confId=10808.

[48] ATLAS Collaboration, Report No. ATLAS-CONF-2012-091.

[49] ATLAS Collaboration, Report No. ATLAS-CONF-2012-168.

[50] CMS Collaboration, Report No. CMS PAS HIG-12-015.

[51] S. Dittmaier *et al.* (LHC Higgs Cross Section Working Group), arXiv:1101.0593.

[52] J. R. Espinosa, M. Muhlleitner, C. Grojean, and M. Trott, J. High Energy Phys. 09 (2012) 126.

[53] M. Raidal and A. Strumia, Phys. Rev. D **84**, 077701 (2011).

[54] J. Alwall, M. Herquet, F. Maltoni, O. Mattelaer, and T. Stelzer, J. High Energy Phys. 06 (2011) 128.

[55] N. D. Christensen and C. Duhr, Comput. Phys. Commun. **180**, 1614 (2009).

[56] A. Pukhov *et al.*, arXiv:hep-ph/9908288.

[57] E. Boos, V. Bunichev, M. Dubinin, L. Dudko, V. Edneral, V. Ilyin, A. Kryukov, V. Savrin, A. Semenov, and A. Sherstnev (CompHEP Collaboration), Nucl. Instrum. Methods Phys. Res., Sect. A **534**, 250 (2004).

[58] K. Arnold *et al.*, arXiv:1107.4038.

[59] G. Fogli, E. Lisi, A. Marrone, D. Montanino, and A. Palazzo, Phys. Rev. D **66**, 053010 (2002).

[60] M. Gonzalez-Garcia and M. Maltoni, Phys. Rep. **460**, 1 (2008).

[61] E. Masso and V. Sanz, arXiv:1211.1320.

[62] See, for instance, L. G. Almeida, E. Bertuzzo, P. A. N. Machado, and R. Z. Funchal, J. High Energy Phys. 11 (2012) 085; E. Bertuzzo, P. A. N. Machado, and R. Zukanovich Funchal, arXiv:1209.6359; N. Arkani-Hamed, K. Blum, R. T. D'Agnolo, and J. Fan, arXiv:1207.4482; H. An, T. Liu, and L.-T. Wang, Phys. Rev. D **86**, 075030 (2012); A. Joglekar, P. Schwaller, and C. E. Wagner, J. High Energy Phys. 12 (2012) 064; N. Arkani-Hamed, K. Blum, R. T. D'Agnolo, and J. Fan, arXiv:1207.4482; H. Davoudiasl, H.-S. Lee, and W. J.

Marciano, Phys. Rev. D **86**, 095009 (2012); M. Voloshin, Phys. Rev. D **86**, 093016 (2012); J. Kearney, A. Pierce, and N. Weiner, Phys. Rev. D **86**, 113005 (2012); S. Dawson and E. Furlan, Phys. Rev. D **86**, 015021 (2012); H. M. Lee, M. Park, and W.-I. Park, J. High Energy Phys. 12 (2012) 037; P. Draper and D. McKeen, Phys. Rev. D **85**, 115023 (2012); A. Akeroyd and S. Moretti, Phys. Rev. D **86**, 035015 (2012); L. Wang and X.-F. Han, arXiv:1209.0376; D. Bertolini and M. McCullough, arXiv:1207.4209; E. J. Chun, H. M. Lee, and P. Sharma, J. High Energy Phys. 11 (2012) 106; W.-F. Chang, J. N. Ng, and J. M. Wu, Phys. Rev. D **86**, 033003 (2012); G. D. Kribs and A. Martin, Phys. Rev. D **86**, 095023 (2012); I. Dorsner, S. Fajfer, A. Greljo, and J. F. Kamenik, J. High Energy Phys. 11 (2012) 130; A. Urbano, arXiv:1208.5782 [Phys. Rev. D (to be published)]; A. Alves, E. Ramirez Barreto, A. Dias, C. A. de S. Pires, F. Queiroz, and P. Rodrigues da Silva, Phys. Rev. D **84**, 115004 (2011); J. Cao, Z. Heng, T. Liu, and J. M. Yang, Phys. Lett. B **703**, 462 (2011); J.-J. Cao, Z.-X. Heng, J. M. Yang, Y.-M. Zhang, and J.-Y. Zhu, J. High Energy Phys. 03 (2012) 086; M. Carena, S. Gori, N. R. Shah, and C. E. Wagner, J. High Energy Phys. 03 (2012) 014; M. Carena, S. Gori, N. R. Shah, C. E. Wagner, and L.-T. Wang, J. High Energy Phys. 07 (2012) 175; R. Sato, K. Tobioka, and N. Yokozaki, Phys. Lett. B **716**, 441 (2012); F. Boudjema and G. D. La Rochelle, arXiv:1208.1952; T. Kitahara, J. High Energy Phys. 11 (2012) 021; K. Schmidt-Hoberg and F. Staub, J. High Energy Phys. 10 (2012) 195; N. Haba, K. Kaneta, Y. Mimura, and R. Takahashi, arXiv:1207.5102; B. Bellazzini, C. Petersson, and R. Torre, Phys. Rev. D **86**, 033016 (2012).

[63] G. J. Gounaris, J. Layssac, J. E. Paschalis, and F. M. Renard, Z. Phys. C **66**, 619 (1995).

[64] G. J. Gounaris, J. Layssac, and F. M. Renard, Phys. Lett. B **332**, 146 (1994).